Journal of Neonatal Surgery
ISSN(Online): 2226-0439
Vol.11 , (2022)
https://www.jneonatalsurg.com

OPEN ACCESS

Polydopamine Nanoparticles Protect Against Nicotine-Induced Male Reproductive Toxicity: An In Vitro Study

Gantimarri Venkatesh Babu[1*]

National Institute of Pharmaceutical Education and Research (NIPER), Balanagar, Hyderabad, Telangana – 500037, India

Corresponding Author:

Gantimarri Venkatesh Babu

Email:ID: venkateshvvgantimarri@gmail.com

Cite this paper as: Gantimarri Venkatesh Babu (2022) Polydopamine Nanoparticles Protect Against Nicotine-Induced Male Reproductive Toxicity: An In Vitro Study..Journal of Neonatal Surgery, 11, 109-123

ABSTRACT

Background: Male infertility affects 45–50% of infertile couples worldwide. Nicotine, the primary toxic alkaloid in tobacco, causes male reproductive toxicity by inducing excessive reactive oxygen species generation, oxidative damage to spermatozoa, and disruption of spermatogenesis. Polydopamine nanoparticles, melanin-mimicking nanomaterials derived from the self-polymerization of dopamine, possess potent antioxidant and ROS-scavenging properties.

Objectives: This study aimed to synthesize and characterize polydopamine nanoparticles and evaluate their protective effects against nicotine-induced sperm cell toxicity in vitro.

Methods: Bare polydopamine nanoparticles were synthesized via a modified Stöber method and characterized using scanning electron microscopy, dynamic light scattering, Fourier transform infrared spectroscopy, and UV-visible spectroscopy. Sperm cells isolated from the cauda epididymis of Swiss albino mice were treated with nicotine and co-incubated with polydopamine nanoparticles (3–100 µM) for 4 hours. Sperm cytotoxicity, head morphology, nuclear maturity, chromatin condensation, acrosomal integrity, DNA fragmentation, and intracellular oxidative stress were assessed.

Results: Polydopamine nanoparticles were spherical, smooth, and uniform (~280 nm; PDI: 0.339). Nicotine significantly increased sperm toxicity and all oxidative damage parameters ($p < 0.0001$ vs. normal control). Co-treatment with polydopamine nanoparticles (3–100 µM) significantly restored sperm viability and reversed all nicotine-induced toxicological endpoints in a concentration-dependent manner ($p < 0.001$ vs. disease control).

Conclusions: Polydopamine nanoparticles effectively mitigate nicotine-induced oxidative damage to sperm cells in vitro, supporting their potential as a therapeutic nanomaterial for drug-induced male reproductive toxicity

Key Words: Polydopamine nanoparticles; nicotine; male reproductive toxicity; oxidative stress; reactive oxygen species; sperm quality; nanomedicine

INTRODUCTION

Infertility has become a prevalent disorder affecting approximately 10–15% of couples trying to conceive, with the majority of these infertility cases originating from highly populated countries [1]. Male infertility factors contribute to approximately 45–50% of these cases, and 7% of men worldwide are diagnosed as infertile [2]. A comprehensive study conducted in the Chongqing region of Southwest China reported that 60% of men had at least one semen characteristic below current World Health Organization reference values [1]. Infertility is one of the apparent harmful effects of tobacco smoking. Approximately one-third of the world's population uses tobacco products daily [2].

There are more than 4,000 chemicals present in tobacco smoke, including hazardous substances such as nicotine, cotinine, lead, alkaloids, cadmium, and other carcinogenic compounds, which complicates the toxicological mechanisms [3]. Nicotine is an alkaloid organic compound found in the leaves of the tobacco plant, constituting approximately 1.5% by weight of commercial cigarette tobacco and approximately 95% of the total alkaloid content. Nicotine is the main toxic component of cigarette smoking, with genotoxic, immunotoxic, as well as reproductive effects in both sexes [4,5]. This psychoactive substance is a natural liquid alkaloid and a volatile base that is colorless, water-soluble, and forms hydro-soluble salts, with cotinine as the major metabolite [6].

The presence of these substances in seminal plasma has been reported, indicating their ability to pass through the blood–testis barrier [7]. Spermatogenesis is highly vulnerable to reproductive toxicants due to continuous cell divisions, sperm cell differentiation, and maturation processes [1]. Studies conducted comparing smokers and non-smokers have indicated reduced semen quality, sperm maturation, spermatozoa function, impaired spermatogenesis, and reproductive hormone system dysfunction in smokers [3,7]. The overall effect of tobacco smoking on fertility is also due to elevated oxidative stress, DNA damage, and cell apoptosis.

Oxidative stress is defined as a pathological imbalance between reactive oxygen species (ROS) and antioxidants. ROS are highly reactive oxygen-derived molecules with unbound electrons. Oxidative stress is one of the crucial pathological mechanisms of nicotine toxicity that results in excessive ROS production, which overwhelms the eliminatory systems of antioxidants [8]. Within safe levels, ROS plays an important role in the acrosomal reaction, sperm capacitation, and spermatozoon–oocyte fusion. However, the causative factors for infertility in 30–80% of men are due to ROS-mediated damage to spermatozoa and decreased levels of seminal total antioxidant capacity [2].

The plasma membrane of spermatozoa is highly vulnerable to ROS-mediated damage and lipid peroxidation due to the ample presence of polyunsaturated fatty acids (PUFAs) [9]. PUFAs contain various double bonds separated by methylene groups, which are sensitive to generating lipid peroxides and aldehydes, associated with reduced motility, viability, structural integrity, and metabolic activity of human sperm [10]. Lipid peroxidation means the oxidative degradation of lipids. Free radicals 'steal' electrons from the lipids in sperm cell membranes, creating cell damage such as changes in structure, accumulation, and dynamics of lipid membranes, leading to a free radical chain reaction mechanism [11].

The lipid peroxidation cascade can be explained in three stages: initiation, propagation, and termination. During the initiation phase, high levels of ROS activate the liberation of PUFAs. Once combined with hydroxyl radicals (•OH), water is generated along with lipid radicals. The propagation stage is characterized by the reaction of unstable lipid radicals with oxygen (O_2), generating peroxyl radicals. A stable end product is formed when the termination phase arises due to reactions of two radicals creating non-radical species [11].

Various electrophilic lipid aldehydes such as 4-hydroxynonenal (4-HNE), malondialdehyde (MDA), and acrolein (ACR) are created, which terminate the reaction. These are powerful electrophiles, forming adducts with several proteins in sperm cells and generating a reduction in spermatozoa function [12]. Testicular damage occurs because of the increased generation of ROS by nicotine, which attacks the PUFAs in the testes' membrane, thus leading to the loss of testicular structure and function. Moreover, the reduction of spermatogenic cells and sperm could be due to interference in testosterone hormone production by nicotine [13].

Nicotine also induces protein oxidation in androgenic enzymes and disrupts testosterone hormone production. Nicotine affects testosterone levels, pituitary gonadotropins, and testicular antioxidant status [12]. Studies on male rats indicate that cigarette smoking and nicotine administration increase prolactin levels and inhibit the release of gonadotropin-releasing hormone (GnRH), thus impairing the gonadotropins follicle-stimulating hormone (FSH) and luteinizing hormone (LH). These hormones control the function of Sertoli and Leydig cells that are critical for initiating and completing spermatogenesis and steroidogenesis in the testis [14]. The internal surfaces of seminiferous tubules are covered by spermatogonia. Sertoli cells, which cover seminiferous tubules, play a pivotal role in the control of germ cell survival and maintenance of spermatogenesis. However, nicotine-induced overproduction of ROS in the testis may override the antioxidant defense mechanisms [15].

The testicular key androgenic enzyme activities, plasma and intratesticular testosterone (ITT) concentrations, and plasma concentration of gonadotropins are significantly reduced by nicotine treatment along with decreased sperm counts and disruption of spermatogenesis [16]. Indeed, it has been shown that ROS inhibits steroidogenesis by interfering with cholesterol transport to mitochondria and/or catalytic function of P450 enzymes. Moreover, ROS also inhibits steroidogenesis during cholesterol transfer by suppression of the steroidogenic acute regulatory (StAR) protein expression [16].

Given the central role of oxidative stress in nicotine-induced reproductive toxicity, antioxidant-based therapeutic strategies represent a rational intervention approach. Nanotechnology offers a promising alternative through the development of nano-antioxidants with superior ROS-scavenging capacity.

Polydopamine nanoparticles (PDA NPs), synthesized by the self-polymerization of dopamine under alkaline conditions, have emerged as a versatile biocompatible nanomaterial [17]. PDA NPs, a biocompatible and biodegradable polymer, have a similar structure and chemical properties to those of melanin [18]. PDA NPs with enriched phenol groups function as a radical scavenger to eliminate ROS generated during inflammatory responses [19]. The typical redox chemistry of catechol endows PDA NPs with the key feature of scavenging a variety of free radicals. On the one hand, catechol can provide hydrogen atoms from the phenolic hydroxyl groups to quench free radicals; on the other hand, catechol can also reduce certain compounds through electron transfer, and the resulting phenoxyl radical can further form stable quinone structures by interacting with the second radical [20].

In addition to directly reacting with ROS as a reducing agent, PDA NPs also regulate ROS generation in mitochondria, which

are considered cellular powerhouses. Specifically, the efficiency of mitochondrial oxidative phosphorylation (OXPHOS) is significantly increased in the presence of PDA NPs, indicating that PDA NPs may increase the efficiency of mitochondrial respiration, hence reducing ROS production [20]. PDA NPs have demonstrated therapeutic efficacy in periodontal disease, acute inflammation-induced injury, and osteoarthritis [19,20,21].

The present study was designed to: (i) synthesize and characterize bare PDA NPs; (ii) establish an in vitro model of nicotine-induced sperm toxicity; and (iii) evaluate the protective efficacy of PDA NPs against nicotine-induced oxidative damage to murine spermatozoa.

2. MATERIALS AND METHODS

2.1 Chemicals and Reagents

Dopamine hydrochloride, nicotine, MTT (3-(4,5-dimethylthiazol-2-yl)-2,5-diphenyl tetrazolium bromide), dimethyl sulfoxide (DMSO), eosin Y, aniline blue, toluidine blue, Coomassie brilliant blue R-250, acridine orange, DAPI, DCFH-DA, and all other reagents were obtained from SRL Chemicals and Sigma-Aldrich (St. Louis, MO, USA). All chemicals were of analytical grade.

2.2 Synthesis of Polydopamine Nanoparticles

Melanin-like PDA NPs were synthesized using a modified Stöber method [22]. Briefly, dopamine hydrochloride (180 mg) was dissolved in deionized water (90 mL) at 50°C under vigorous stirring. NaOH solution (760 µL of 1 M) was injected to initiate auto-oxidative polymerization. After aging for 5 hours, PDA NPs were collected by centrifugation at 18,000 rpm, washed with deionized water several times, and lyophilized.

2.3 Characterization of PDA NPs

The surface morphology of synthesized PDA NPs was measured using scanning electron microscopy (SEM). The hydrodynamic size and polydispersity index (PDI) were determined using dynamic light scattering (DLS) (Zetasizer Nano ZS90, Malvern, UK). Functional groups were characterized by Fourier transform infrared spectroscopy (FTIR) (PerkinElmer spectrophotometer). UV-visible absorbance spectra were recorded on a Cary 300 Bio UV-vis spectrophotometer (400–800 nm).

2.4 Animals

Male Swiss albino mice (age: 6–8 weeks; body weight: 25–30 g) were housed under controlled conditions (22 ± 2°C; humidity 45–65%; 12 h light/dark cycle) with free access to food and water. All procedures were conducted in accordance with CPCSEA guidelines following approval from the Institutional Animal Ethics Committee, NIPER Hyderabad.

2.5 Epididymal Sperm Isolation and In Vitro Treatment

Cauda epididymides were excised and placed in Hank's Balanced Salt Solution (HBSS). Epididymides were minced, and the sperm solution was centrifuged at 1,000 rpm for 3 minutes. Sperm concentration was adjusted to 2×10^6 cells/mL [23]. Sperm suspensions were incubated with nicotine (1.2 µM, IC_{50}) alone or combined with PDA NPs (3, 10, 30, or 100 µM) for 4 hours at 37°C.

2.6 Sperm Head Morphology

For sperm head morphology, 0.5 mL of sperm suspension and 0.5 mL of 2% eosin solution were mixed and kept for 1 hour. Smears were prepared, air-dried, and fixed with absolute methanol for 3 minutes. One hundred sperm cells per sample were examined to determine morphological abnormalities [24].

2.7 Sperm Viability Assay

The MTT assay was used to assess viability. Ten microliters of MTT stock solution (5 mg/mL) were added to each tube containing sperm suspension and incubated at 37°C for 1 hour. The precipitate was dissolved in 200 µL DMSO, and absorbance was measured at 570 nm [25].

2.8 Epididymal Sperm Nuclear Maturity

Air-dried fixed smears were stained for 7 minutes with 5% aniline blue (pH 3.5). One hundred sperm cells per slide were counted to determine the percentage of immature (blue-stained) sperm cells [26].

2.9 Sperm Chromatin Condensation

Air-dried smears were fixed in ethanol–acetone (1:1) at 4°C for 1 hour, hydrolyzed in 0.1 N HCl at 4°C for 5 minutes, and stained with 0.05% toluidine blue (pH 3.5) for 5 minutes. Sperm with good chromatin integrity appeared light blue; those with diminished integrity appeared deep violet [27].

2.10 Evaluation of Acrosomal Integrity

Smears were stained with 0.5% Coomassie brilliant blue for 90 seconds. The acrosome was defined as intact (uniform dark-

blue staining), damaged (patchy staining), or non-intact (no staining) [28].

2.11 Halosperm Technique

The sperm chromatin dispersion (SCD) test was performed as described by Fernández et al. [29]. Sperm were mixed with 1% low-melting-point agarose, placed on pre-coated slides, and treated with acid denaturation solution (0.08 N HCl) for 7 minutes. After lysis and dehydration, cells were stained with DAPI and observed under a fluorescence microscope.

2.12 Assessment of Intracellular Oxidative Stress

Spermatozoa were treated with 5 µM H_2DCFDA for 30 minutes. The percentage of DCF-positive spermatozoa was evaluated by fluorescence microscopy [30].

2.13 Histopathological Examination

Testes were fixed in 10% neutral buffered formalin, processed, embedded in paraffin, sectioned at 5 µm, and stained with hematoxylin and eosin [31].

2.14 Statistical Analysis

Data are expressed as mean ± SEM. One-way ANOVA with Tukey's multiple comparison test was performed using GraphPad Prism 8.0. Significance levels: $p < 0.05$, $p < 0.01$, $p < 0.001$, $p < 0.0001$ vs. normal control; $p < 0.1$, $p < 0.01$, $p < 0.001$, $p < 0.0001$ vs. nicotine-treated group.

3. RESULTS

3.1 Characterization of PDA NPs

3.1.1 Scanning Electron Microscopy

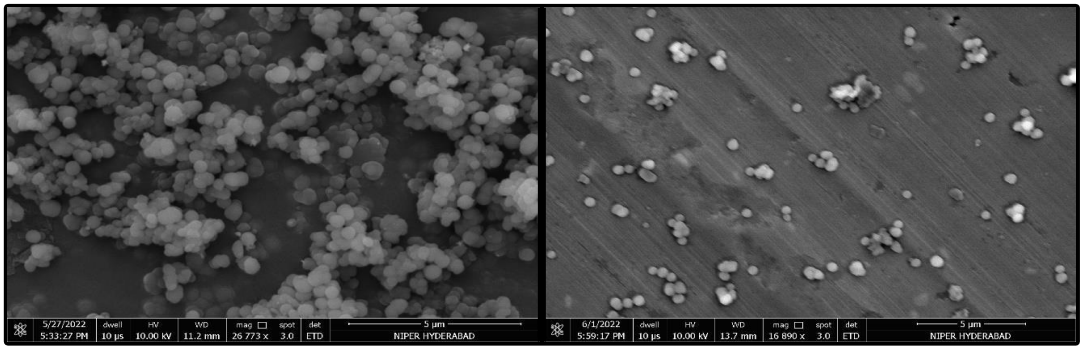

Figure 1: Scanning Electron Microscope (SEM) images of PDA NPs showing uniform, smooth and spherical shape with an average diameter of 280.4 nm

The surface morphology and size of synthesized PDA NPs were measured using SEM. PDA NPs existed in smooth, uniform, and spherical shapes with a mean particle size of 280.4 nm (Figure 1).

3.1.2 Dynamic Light Scattering

DLS results revealed that the average hydrodynamic diameter of PDA NPs was approximately 284 nm, with a polydispersity index of 0.339.

3.1.3 Fourier Transform Infrared Spectroscopy

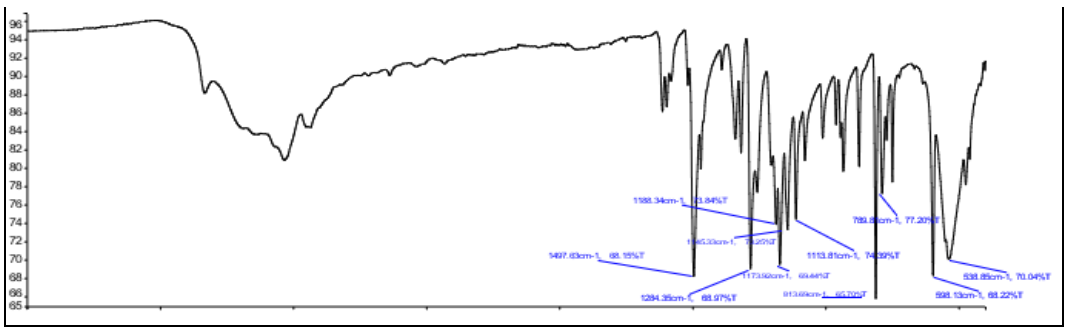

Figure 2: FTIR of Dopamine hydrochloride. The peak at approximately 3336 cm^{-1} corresponds to the stretching vibrations of –OH and N–H bonds. The peaks at 1591 cm^{-1}, 1497 cm^{-1}, and 1284 cm^{-1} were attributed to the C = O, C = C, and C-O bonds, respectively

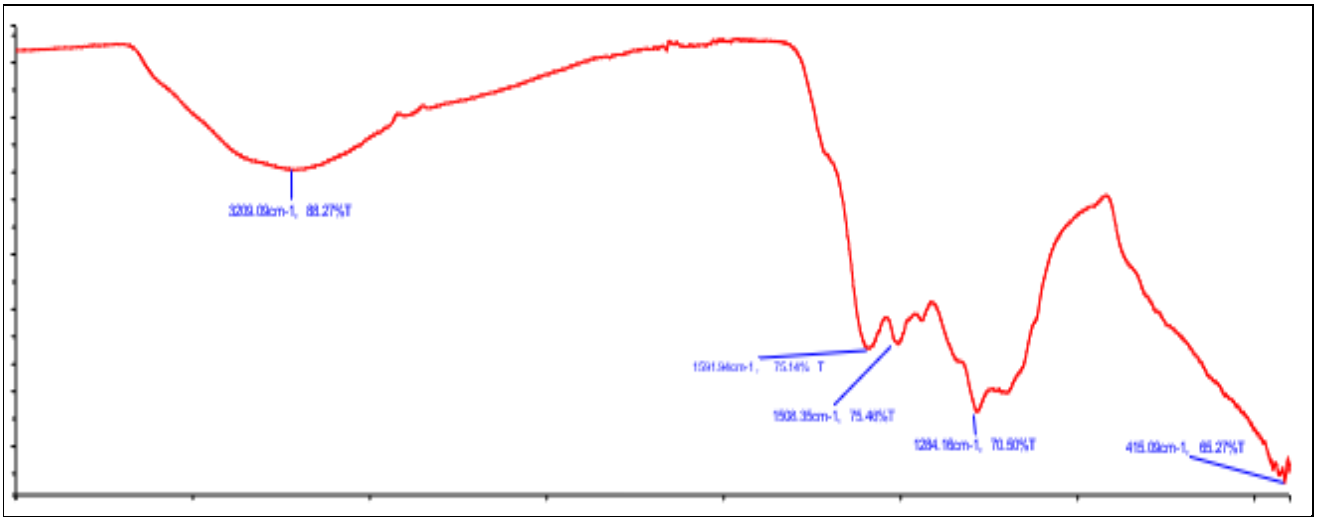

Figure 3: FTIR of PDA NPs. The broad band from 3000-3600 cm^{-1} is attributed to the stretching modes of N-H and O-H bonds. Moreover, the peak at 1591 and 1508 cm^{-1} is due to the stretching of aromatic C=C bonds of indole, and the peak at 1284 cm^{-1} was corresponding to C-N bending in indolequinone. The absorption band at approximately 700 cm^{-1} as markedly weaker than that of dopamine, suggesting the decrease in aromatic structures as well as the expected polymerization in the PDA NPs

FTIR spectroscopy confirmed the successful formation of PDA NPs (Figures 6 and 7). The broad band from 3000–3600 cm^{-1} was attributed to N–H and O–H stretching modes. The absorption band at approximately 700 cm^{-1} was markedly weaker than that of dopamine, suggesting the expected polymerization.

3.1.4 UV-Visible Absorbance

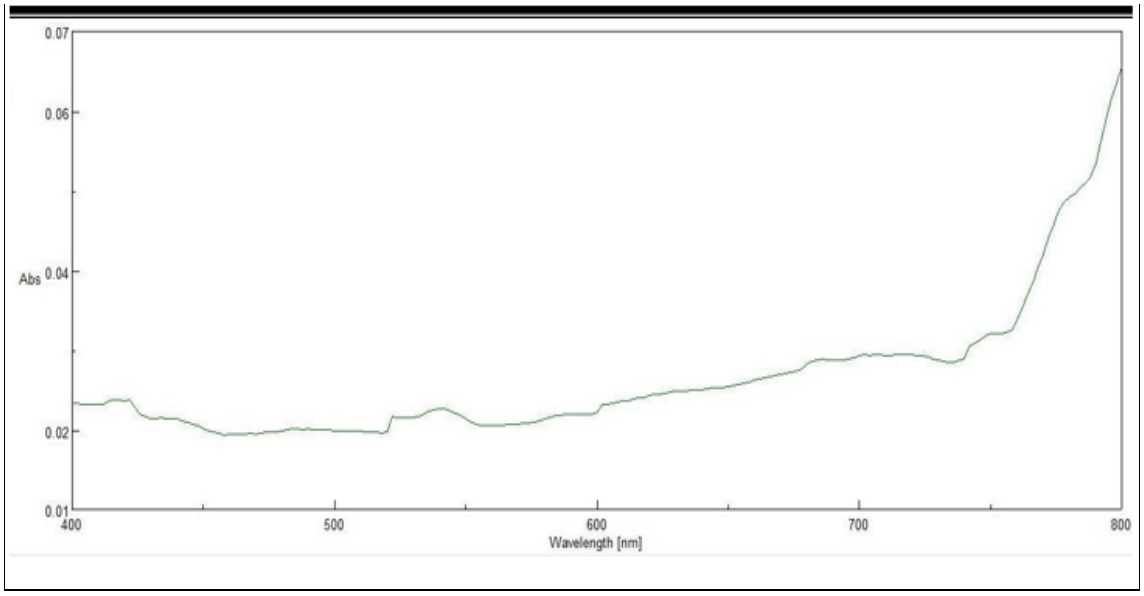

Figure 4: UV-Visible spectroscopy of PDA NPs. UV-visible spectrum showed broad absorption of PDA NPs in UV-visible range confirming its presence

UV-visible spectrum showed broad absorption of PDA NPs in the 400–800 nm range (Figure 8).

3.2 Histopathological Examination

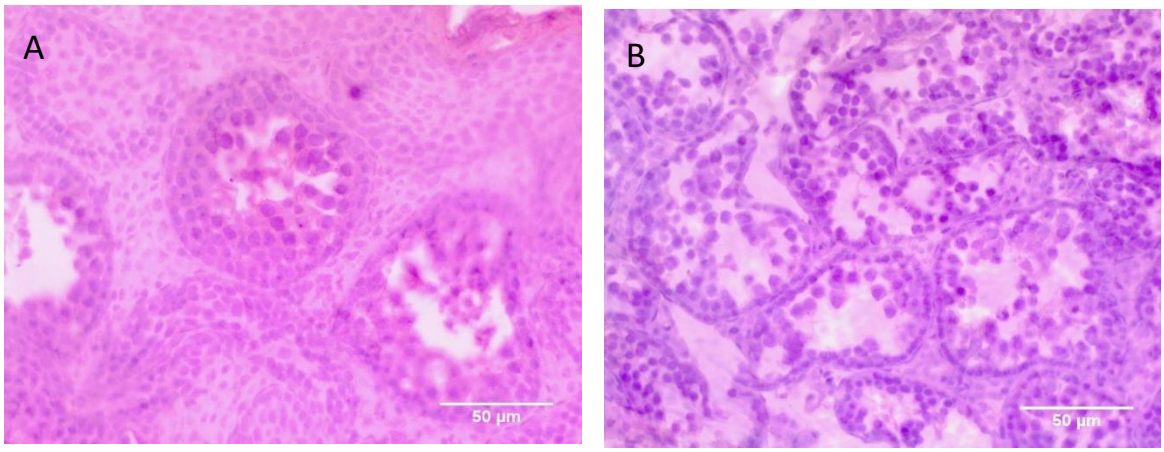

Figure 5: Haematoxylin & Eosin staining of mice testes which have not attained puberty. A: unopened vacuoles in the seminiferous tubules, B: underdeveloped Sertoli cells in the seminiferous tubules without spermatozoa

H&E staining revealed that the mice had not attained puberty, as evidenced by underdeveloped Sertoli cells and the absence of spermatozoa in the seminiferous tubules (Figure 5).

3.3 Effect of PDA NPs Against Nicotine-Induced Defects in Sperm Head Morphology

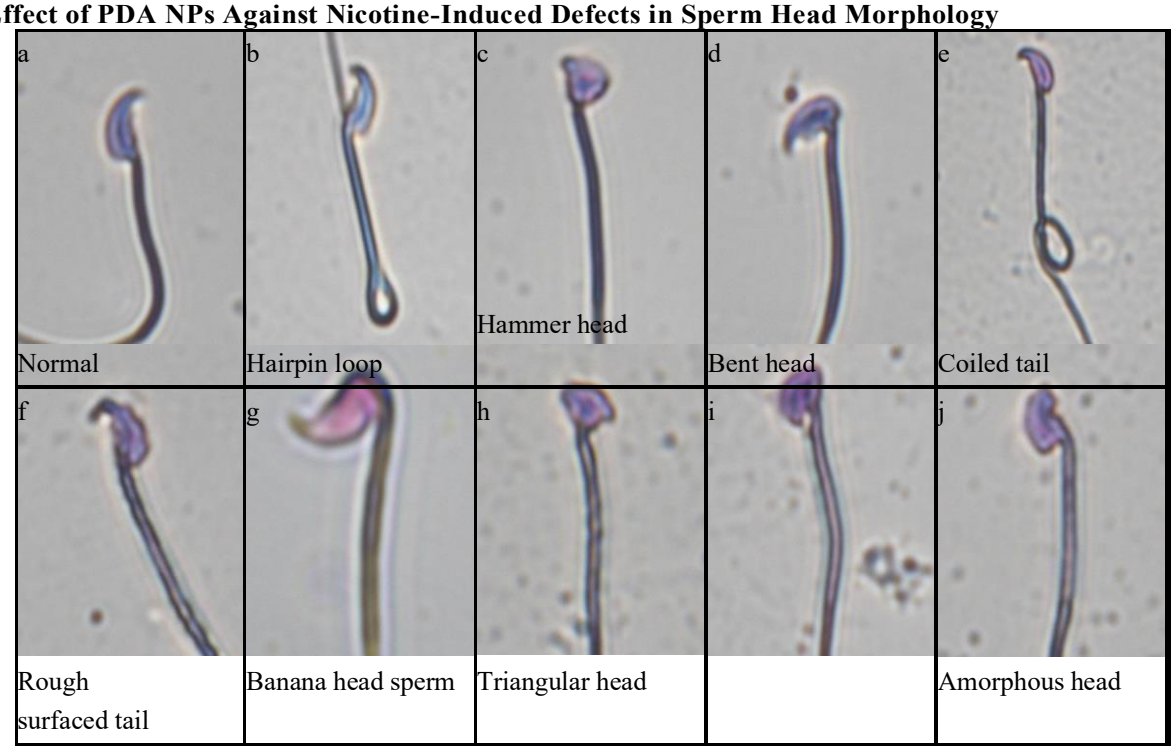

Figure 6: Effect of polydopamine nanoparticles against nicotine-induced defects in sperm head morphology (60X magnification). Normal sperm (a), hairpin loop (b), hammerhead (c), bent head (d), coiled tail (e), rough surfaced tail (f), banana head sperm (g), triangular head (h and i) and amorphous head (j)

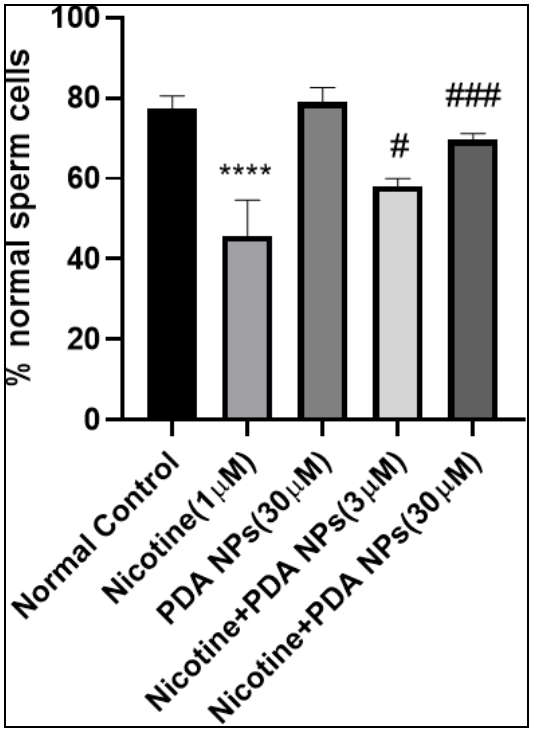

Figure 7: Graphical representation of the percentage of abnormal sperms when treated with nicotine and PDA NPs. At least 100 sperms were counted and expressed as percentage of abnormal cells. The data is expressed as mean ± SEM and analyzed by one-way ANOVA with Tukey's multiple comparison test; ****p<0.0001 vs NC, $^{\#}$p<0.1 vs nicotine, $^{\#\#\#}$p<0.01 vs nicotine

Different types of sperm head morphologies caused by nicotine are shown in Figure 10. Nicotine treatment significantly increased the percentage of abnormal sperm ($p < 0.0001$ vs. normal control). Co-treatment with PDA NPs significantly reduced abnormal sperm in a concentration-dependent manner ($p < 0.01$ vs. nicotine) (Figure 7).

3.4 Effect of Nicotine on Cytotoxicity

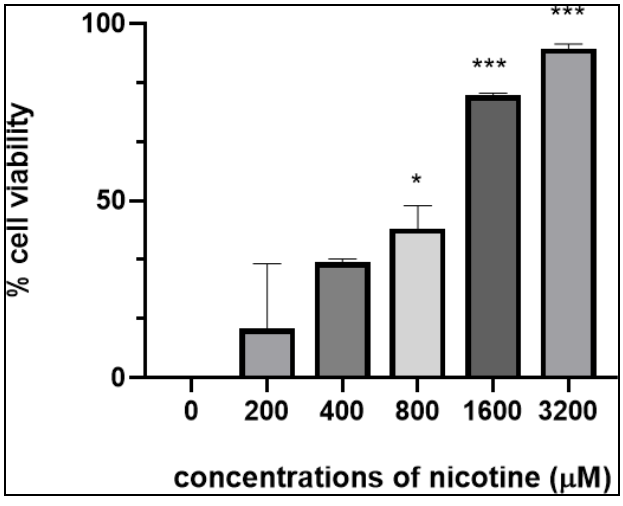

Figure 8: Effect of different concentrations of nicotine treatment for 4 h on cytotoxicity of sperm cells using MTT assay. IC50 value was found to be at 1.2 µM. Data was expressed as mean ± SEM (n=5-6) and analyzed by one-way ANOVA with Tukey's multiple comparison test, ****p<0.0001vs NC

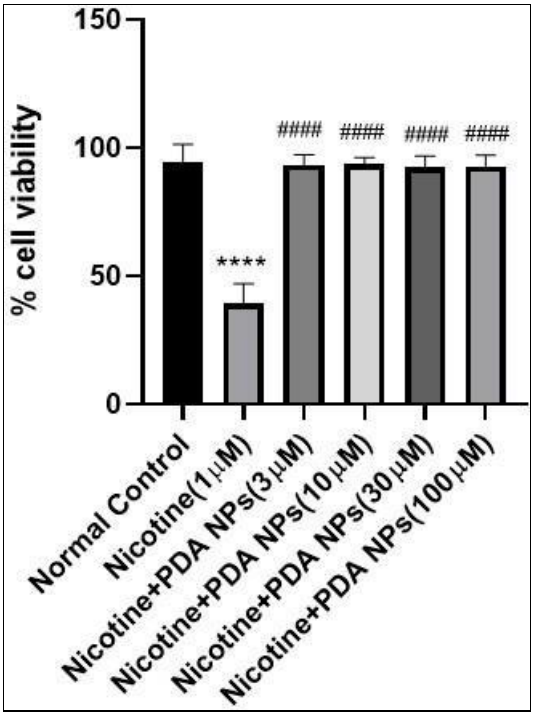

Figure 9: Graphical representation of sperm cell viability when treated with nicotine and different concentrations of PDA NPs. Data was expressed as mean ± SEM (n=5-6) and analyzed by one-way ANOVA with Tukey's multiple comparison test, ****p<0.0001vs NC, ####p<0.001vs DC

The IC_{50} of nicotine was 1.2 µM (Figure 8). Co-treatment with PDA NPs significantly restored sperm viability ($p < 0.001$ vs. disease control) (Figure 9).

3.5 Epididymal Sperm Nuclear Maturity

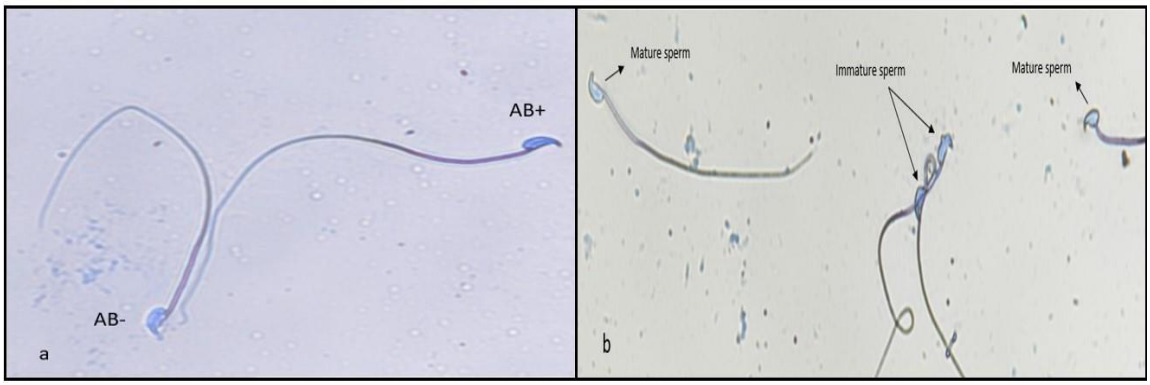

Figure 10: Epididymal sperm nuclear maturity. Unstained sperms (AB-) indicates that the sperms contain protamine-rich nuclei and the sperms with blue color indicates immature sperms (AB+) containing lysine-rich nuclei (60X magnification)

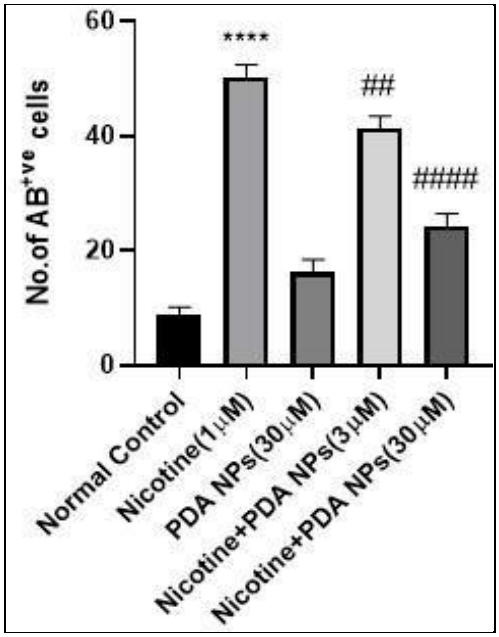

Figure 11: Graphical representation of the number of cells have taken up aniline blue stain which indicates immature sperm cells. At least 100 sperms were scored per group. The data is expressed as mean ± SEM and analyzed by one-way ANOVA with Tukey's multiple comparison test; ****p<0.0001 vs NC, $^{\#\#}$p<0.01 vs nicotine+PDA NPs(3 µM), $^{\#\#\#\#}$p<0.0001 vs nicotine+PDA NPs(30 µM)

Nicotine significantly increased immature sperm (AB^+) ($p < 0.0001$ vs. NC). PDA NPs at 30 µM showed marked protection ($p < 0.0001$ vs. nicotine) (Figures 10 and 11).

3.6 Sperm Chromatin Condensation

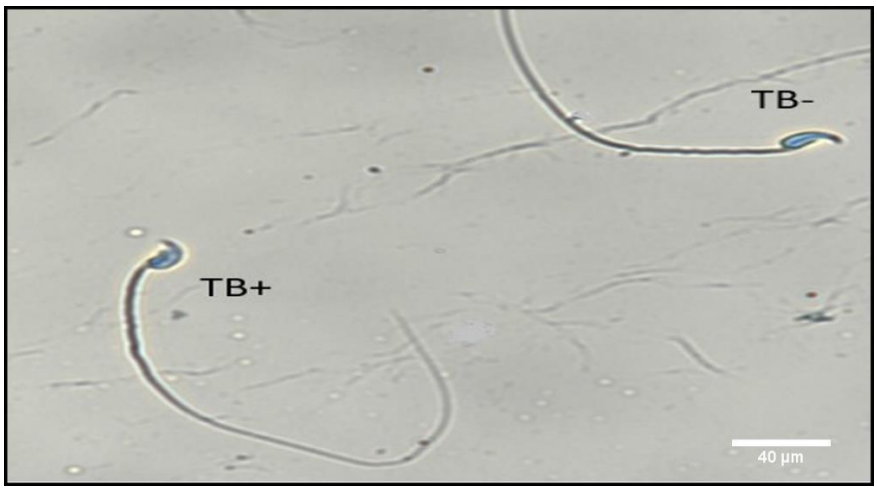

Figure 12: Sperm chromatin condensation. sperms with light blue (TB-) colored head indicates good chromatin integrity whereas the sperms with purple color (TB+) indicates diminished integrity (60X magnification)

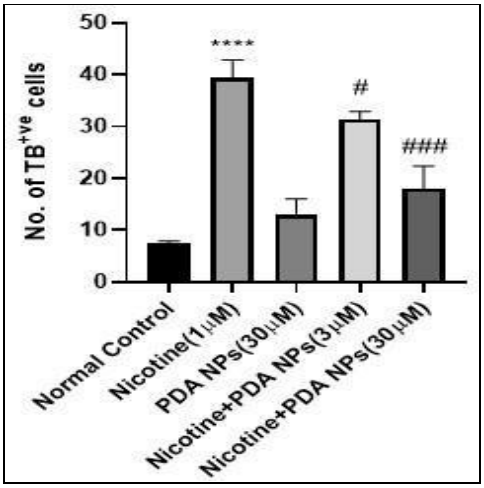

Figure 13: Graphical representation of the number of sperm cells taken up the toluidine stain when treated with nicotine and PDA NPs. At least 100 were scored per group. The data is expressed as mean ± SEM and analyzed by one-way ANOVA with Tukey's multiple comparison test; ****p<0.0001 vs NC, $^{\#\#}$p<0.01 vs nicotine+PDA NPs(3 µM), $^{\#\#\#\#}$p<0.0001 vs nicotine+PDA NPs(30 µM)

Nicotine significantly increased abnormal chromatin condensation ($p < 0.0001$ vs. NC). PDA NPs at 30 µM showed marked protection ($p < 0.0001$ vs. nicotine) (Figures 12 and 13).

3.7 Evaluation of Acrosomal Integrity

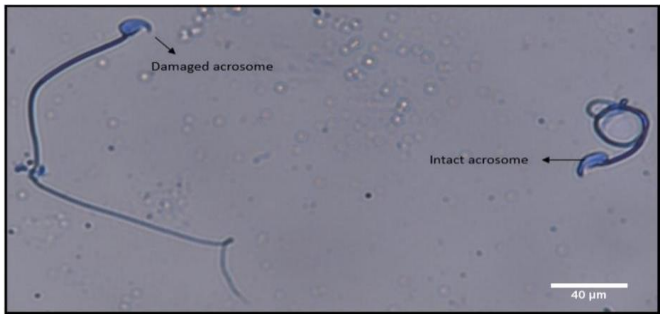

Figure 14: Evaluation of acrosomal integrity. sperms showing dark-blue staining of the entire acrosome region, has intact acrosome and sperms with patchy chromosome indicates damaged acrosome (60X magnification)

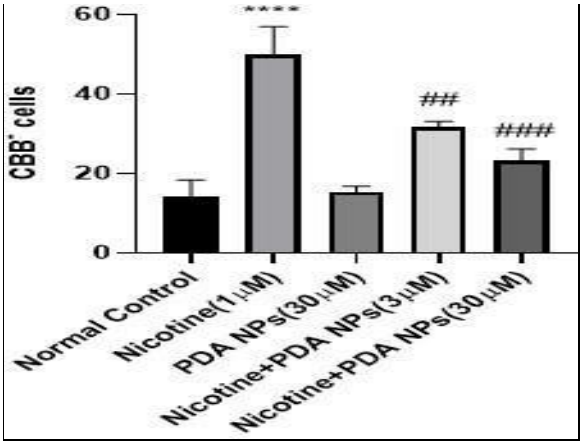

Figure 15: Graphical representation of the no, of cells have damaged acrosome integrity (CBB^{-ve}) treated with nicotine and PDA NPs. At least 100 sperm cells were scored for abnormal acrosomal integrity per group. The data is expressed as mean ± SEM and analyzed by one-way ANOVA with Tukey's multiple comparison test; ****p<0.0001 vs NC, $^{\#\#}$p<0.01 vs nicotine+PDA NPs(3 µM), $^{\#\#\#\#}$p<0.0001 vs nicotine+PDA NPs(30 µM)

Nicotine significantly increased acrosomal damage ($p < 0.0001$ vs. NC). PDA NPs at 30 µM showed significant protection ($p < 0.001$ vs. nicotine) (Figures 14 and 15).

3.8 Halosperm Technique

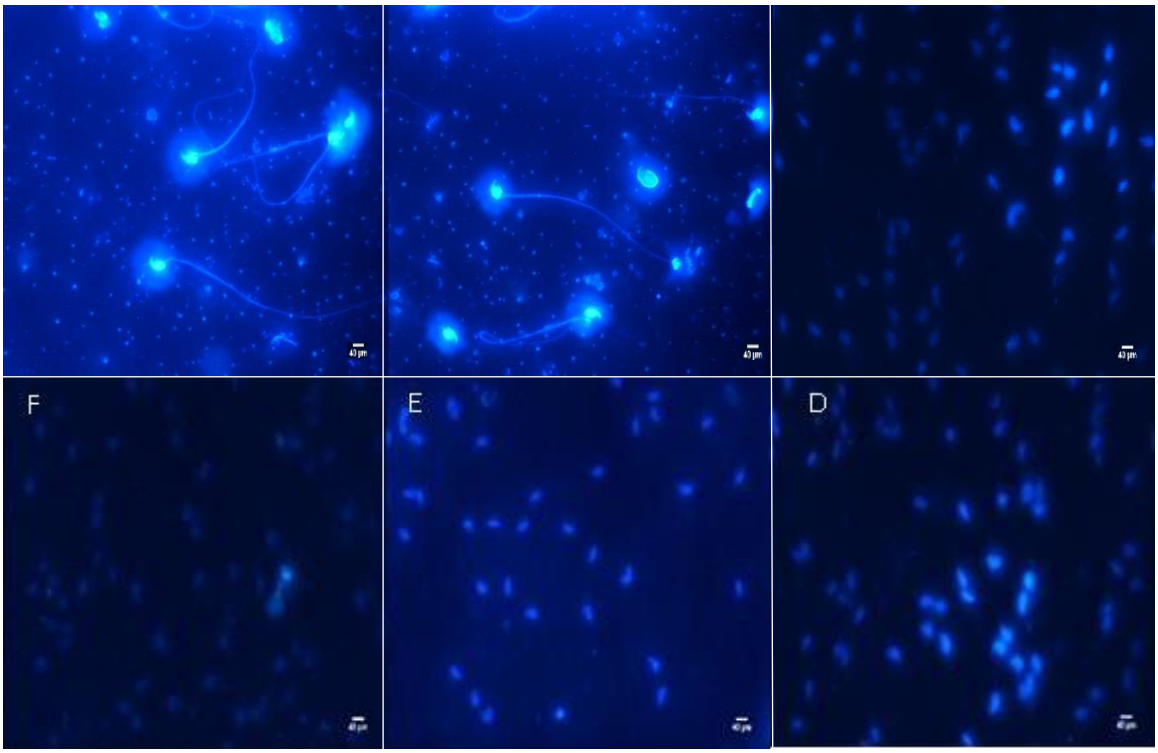

Figure 16: Halosperm technique. (A&B) represent sperms with unfragmented DNA (large halos). (C&D) represent medium halos and (E&F) represent no halos indicating that the sperm cells contain fragmented DNA

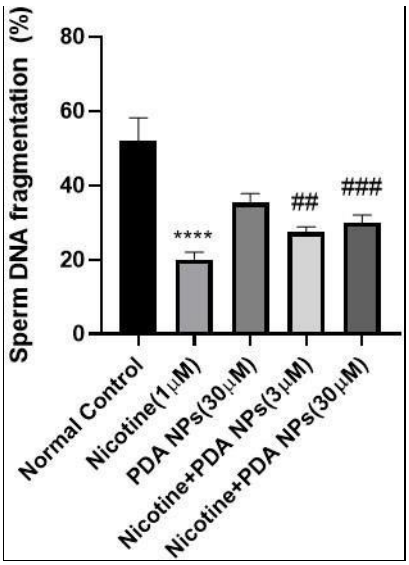

Figure 17: Graphical representation of the number of sperm cells with DNA fragmentation cells per group. At least 100 sperms were counted. The data is expressed as mean ± SEM and analyzed by one-way ANOVA with Tukey's multiple comparison test; ****p<0.0001 vs NC, $^{###}$p<0.001 vs nicotine+PDA NPs(3 µM), $^{##}$p<0.01 vs nicotine+PDA NPs(30 µM)

Nicotine significantly increased DNA fragmentation ($p < 0.0001$ vs. NC). Co-treatment with PDA NPs significantly reduced

DNA fragmentation (Figures 16 and 17).

3.9 Assessment of Intracellular Oxidative Stress

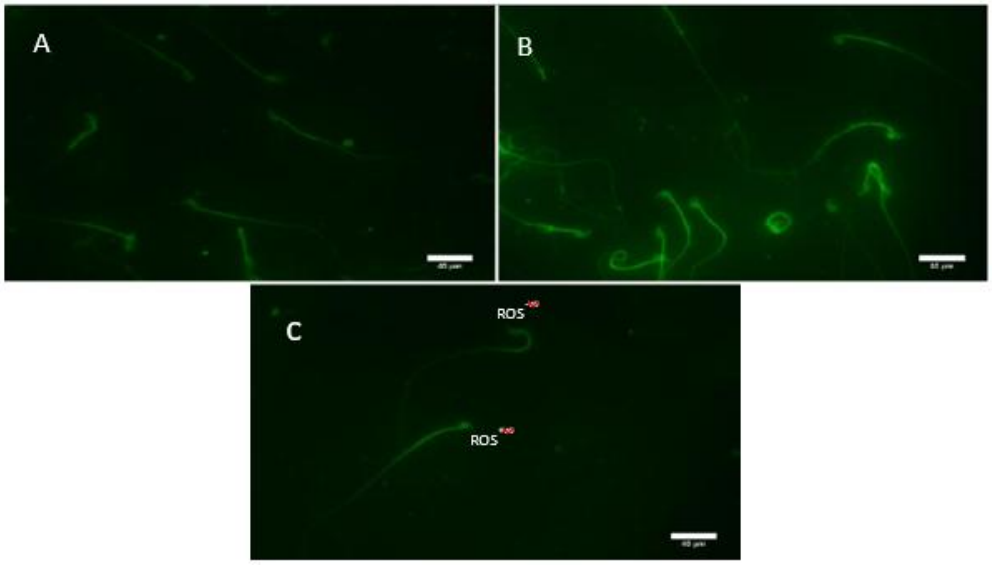

Figure 18: Assessment of intracellular oxidative stress by DCFDA staining. The intensity of the green fluorescence of sperm cells is directly proportional to the ROS levels. A: sperms with less ROS levels, B: sperms with more ROS levels, C: ROS^{-ve} sperm with less ROS, ROS^{+ve} sperm with intense green fluorescence indicating more ROS

DCFDA staining revealed that nicotine treatment markedly increased ROS levels, while PDA NPs co-treatment significantly reduced ROS-positive sperm cells (Figure 18).

4. DISCUSSION

Nicotine is a toxic alkaloid extracted from tobacco plants, comprising about 1.5% by weight in commercial cigarette tobacco and about 95% of the total alkaloid content [4]. It exerts reproductive toxicity through mitochondrial respiratory chain disruption, leading to elevated intracellular ROS that attack PUFAs in sperm plasma membranes, initiating lipid peroxidation cascades that generate reactive aldehydes (MDA, 4-HNE, ACR) [12,32]. Testicular tissue possesses a high amount of unsaturated fatty acids; therefore, the testicles may be an environment with high ROS production [33]. Due to the relatively insufficient blood flow in the testis, testicles are very susceptible to hypoxia and oxidative stress [34].

These electrophilic lipid aldehydes form adducts with several proteins in sperm cells, generating a reduction in spermatozoa function [12]. Moreover, the reduction of spermatogenic cells and sperm could be due to interference in testosterone hormone production by nicotine. Nicotine also affects testosterone levels, pituitary gonadotropins, and testicular antioxidant status [35]. The present study confirmed all these effects following nicotine treatment at 1.2 µM (IC_{50}), consistent with previously published literature [5, 16,36].

The protective effect of PDA NPs against nicotine-induced male reproductive toxicity was evaluated using various in vitro techniques. PDA NPs, an emerging versatile biopolymer produced by self-polymerization of dopamine, have attracted considerable attention in biomedical applications by virtue of their excellent biocompatibility and intriguing ROS-scavenging capacity [20].

The efficacy of PDA NPs is attributable to their dual ROS-scavenging mechanism. On the one hand, catechol moieties donate hydrogen atoms from phenolic hydroxyl groups to quench free radicals; on the other hand, catechol reduces oxidizing species through electron transfer to form stable quinone structures [20]. Owing to the abundant phenolic groups, PDA NPs possess ROS-scavenging properties and have been applied in alleviating ROS-mediated injury and inflammation. Beyond direct scavenging, PDA NPs improve mitochondrial OXPHOS efficiency, thereby reducing endogenous ROS generation at its source [20]. This dual action likely accounts for the comprehensive protection observed across all endpoints in the present study.

The preservation of acrosomal integrity, nuclear maturity, and chromatin condensation by PDA NPs is particularly significant from a fertility perspective. Acrosomal damage impairs the sperm–zona pellucida interaction essential for fertilization [37]. Impaired protamination (histone retention) renders spermatozoa susceptible to further ROS-mediated damage [15]. The aniline blue staining results showed that nicotine treatment significantly increased the percentage of immature sperm, whereas PDA NPs co-treatment reduced this percentage. Similarly, toluidine blue staining revealed that PDA NPs preserved

chromatin condensation. PDA NPs' ability to normalize all these parameters underscores their comprehensive protective mechanism.

The DNA fragmentation data, assessed by the validated Halosperm/SCD technique, further highlights the genoprotective capacity of PDA NPs. Elevated sperm DNA fragmentation is an established predictor of male infertility, implantation failure, and early pregnancy loss [38]. Therefore, the significant reduction of nicotine-induced DNA fragmentation by PDA NPs observed in this study has important clinical implications.

The DCFDA staining results directly confirmed that PDA NPs reduce intracellular ROS levels in nicotine-treated sperm cells [30]. The intense green fluorescence observed in nicotine-treated sperm indicated high ROS levels, whereas PDA NPs co-treatment markedly reduced fluorescence intensity. This finding directly supports the hypothesis that PDA NPs exert their protective effects primarily through ROS scavenging.

It has already been reported that PDA NPs ameliorate acute inflammation-induced injury, osteoarthritis, and periodontal disease by scavenging reactive oxygen species and reducing oxidative stress [19,20,21]. In the present study, incubation of PDA NPs with sperm cells treated with nicotine was found to protect chromatin integrity, acrosomal integrity, reduce intracellular oxidative stress, and decrease the incidence of sperm with head abnormalities.

Previous studies have investigated various antioxidants for nicotine-induced reproductive toxicity. Mohamed and Abdelrahman (2019) reported that zinc oxide nanoparticles protected testicular and epididymal structure in nicotine-treated rats [7]. Seema et al. (2007) showed that selenium protected against nicotine-induced testicular toxicity [39]. Mosbah et al. (2015) demonstrated that green tea extract protected against nicotine-induced reproductive toxicity [36]. Jalili et al. (2017) reported the protective effect of gallic acid on nicotine-induced testicular toxicity [40]. However, the present study is the first to demonstrate the protective effects of PDA NPs against nicotine-induced sperm toxicity in vitro across multiple comprehensive endpoints.

An important limitation of this study is the in vitro nature of the experiments. While in vitro sperm models provide mechanistic insight, they do not fully recapitulate the in vivo testicular microenvironment. Therefore, comprehensive in vivo experiments in Swiss albino mice are planned with nicotine (2 mg/kg, I.P.) and PDA NPs (1 and 3 mg/kg, I.P.) administered daily for 28 days, followed by assessment of biochemical, hormonal, histopathological, and sperm parameters.

5. CONCLUSION

This study demonstrates that polydopamine nanoparticles effectively protect spermatozoa against nicotine-induced oxidative toxicity in vitro. PDA NPs significantly reversed nicotine-induced defects in sperm viability, morphology, nuclear maturity, chromatin condensation, acrosomal integrity, DNA fragmentation, and intracellular ROS levels. These beneficial effects are attributed to the potent ROS-scavenging properties of PDA NPs arising from their enriched phenolic (catechol) groups. The comprehensive protection observed across multiple sperm quality parameters suggests that PDA NPs hold promise as a therapeutic nanomaterial for drug-induced male reproductive toxicity.

Acknowledgements

The authors gratefully acknowledge Dr. Shasi Bala Singh (Director, NIPER Hyderabad) and all faculty members of the Department of Biological Sciences for their support and guidance. The authors also acknowledge Ms. Priyanka Devi, Ms. Shrilekha Chilvery, Ms. Geetanjali Devabattula, and Mr. Biswajit Panda for their support.

Declaration of Competing Interest

The authors declare no conflict of interest.

REFERENCES

[1] J.P. Bonde, Male reproductive organs are at risk from environmental hazards, Asian J. Androl. 12 (2010) 152–156.

[2] E.P.P. Evans et al., Male subfertility and oxidative stress, Redox Biol. 46 (2021) 102071.

[3] J.B. Dai, Z.X. Wang, Z.D. Qiao, The hazardous effects of tobacco smoking on male fertility, Asian J. Androl. 17 (2015) 954–960.

[4] L. Marinucci et al., Effects of nicotine on porcine pre-pubertal Sertoli cells, Toxicol. In Vitro 67 (2020) 104882.

[5] A. ben Saad et al., Nicotine-induced oxidative stress, testis injury, AChE inhibition, Inflammopharmacology 28 (2020) 939–948.

[6] Gandini et al., The in-vitro effects of nicotine and cotinine on sperm motility, (1997).

[7] D.A. Mohamed, S.A. Abdelrahman, The possible protective role of zinc oxide nanoparticles on testicular

structure in nicotine-treated rats, Cell Tissue Res. 375 (2019) 543–558.

[8] S. Bisht, M. Faiq, M. Tolahunase, R. Dada, Oxidative stress and male infertility, Nat. Rev. Urol. 14 (2017) 470–485.

[9] S.H. Lee et al., Effect of nicotinic acid on the plasma membrane function and polyunsaturated fatty acids composition during cryopreservation in boar sperm, Reprod. Domest. Anim. 54 (2019) 1251–1257.

[10] Y. Nemoto, N. Inaba, Testis: anatomy, physiology and pathology.

[11] I.P. Oyeyipo, Y. Raji, A.F. Bolarinwa, Antioxidant profile changes in reproductive tissues of rats treated with nicotine, J. Hum. Reprod. Sci. 7 (2014) 41–46.

[10] S. Bisht et al., Oxidative stress and male infertility, Nat. Rev. Urol. 14 (2017) 470–485.

[11] K. Aydos, M.C. Güven, B. Can, A. Ergün, Nicotine toxicity to the ultrastructure of the testis in rats.

[12] P.P. Vescovi et al., Chronic effects of marihuana smoking on luteinizing hormone, follicle-stimulating hormone and prolactin levels in human males, (1992).

[13] W.H. Nesseim, H.S. Haroun, E. Mostafa, M.F. Youakim, T. Mostafa, Effect of nicotine on spermatogenesis in adult albino rats, Andrologia 43 (2011) 398–404.

[14] K. Jana, P.K. Samanta, D. Kumar De, Nicotine diminishes testicular gametogenesis, steroidogenesis, and steroidogenic acute regulatory protein expression in adult albino rats, Toxicol. Sci. 116 (2010) 647–659.

[15] H. Zhao et al., Polydopamine nanoparticles for the treatment of acute inflammation-induced injury, Nanoscale 10 (2018) 6981–6991.

[16] J. Hu et al., Polydopamine free radical scavengers, Biomater. Sci. 8 (2020) 4940–4950.

[17] X. Bao, J. Zhao, J. Sun, M. Hu, X. Yang, Polydopamine nanoparticles as efficient scavengers for reactive oxygen species in periodontal disease, ACS Nano 12 (2018) 8882–8892.

[18] X. Wang et al., Polydopamine nanoparticles as dual-task platform for osteoarthritis therapy, Chem. Eng. J. 417 (2021) 129284.

[19] H. Zhao et al., Polydopamine nanoparticles for the treatment of acute inflammation-induced injury, Nanoscale 10 (2018) 6981–6991.

[20] K.Y. Ju, Y. Lee, S. Lee, S.B. Park, J.K. Lee, Bioinspired polymerization of dopamine to generate melanin-like nanoparticles, Biomacromolecules 12 (2011) 625–632.

[21] G.P. Kumar, M. Laloraya, P. Agrawal, M.M. Laloraya, The involvement of surface sugars of mammalian spermatozoa in epididymal maturation, Andrologia 22 (1990) 184–194.

[22] K. Bamba, Evaluation of acrosomal integrity of boar spermatozoa by bright field microscopy using an eosin–nigrosin stain, Theriogenology (1988).

[23] F. Eskandari, H.R. Momeni, Protective effect of silymarin on viability, motility and mitochondrial membrane potential of ram sperm treated with sodium arsenite, (2016).

[24] G. Najafi, F. Farokhi, A.S. Jalali, Z. Akbarizadeh, Protection against cyclosporine-induced reprotoxicity by Satureja khuzestanica essential oil in male rats.

[25] T. Ajina et al., Assessment of human sperm DNA integrity using two cytochemical tests: acridine orange test and toluidine blue assay, Andrologia 49 (2017) e12765.

[26] F. Eskandari, H.R. Momeni, Silymarin protects plasma membrane and acrosome integrity in sperm treated with sodium arsenite, Int. J. Fertil. Steril. 10 (2016) 94–101.

[27] J.L. Fernández et al., The sperm chromatin dispersion test: a simple method for the determination of sperm DNA fragmentation, J. Androl. 24 (2003) 59–66.

[28] S. sadat Taherian, R. Khayamabed, M. Tavalaee, M.H. Nasr-Esfahani, Alpha-lipoic acid minimises reactive oxygen species-induced damages during sperm processing, Andrologia 51 (2019) e13314.

[29] M.A. Autifi et al., Effect of nicotine on the testis of adult albino rat and the possible protective effect of vitamin E, Nat. Sci. 15 (2017) 13–19.

[30] M. Arabi, Nicotinic infertility: assessing DNA and plasma membrane integrity of human spermatozoa, Andrologia 36 (2004) 305–310.

[31] N. Asadi, M. Bahmani, A. Kheradmand, M. Rafieian-Kopaei, The impact of oxidative stress on testicular function and the role of antioxidants in improving it: a review, J. Clin. Diagn. Res. 11 (2017) IE01–IE05.

[32] O. Miró et al., Smoking disturbs mitochondrial respiratory chain function and enhances lipid peroxidation on

human circulating lymphocytes, Carcinogenesis 20 (1999) 1331–1336.

[33] L. Marinucci et al., Effects of nicotine on porcine pre-pubertal Sertoli cells: An in vitro study, Toxicol. In Vitro 67 (2020) 104882.

[34] R. Mosbah, M.I. Yousef, A. Mantovani, Nicotine-induced reproductive toxicity, oxidative damage, histological changes and haematotoxicity in male rats, Exp. Toxicol. Pathol. 67 (2015) 253–259.

[35] . Eskandari, H.R. Momeni, Silymarin protects plasma membrane and acrosome integrity, Int. J. Fertil. Steril. 10 (2016) 94–101.

[36] S. Cankut, T. Dinc, M. Cincik, G. Ozturk, B. Selam, Evaluation of sperm DNA fragmentation via Halosperm technique and TUNEL assay before and after cryopreservation, Reprod. Sci. 26 (2019) 1575–1581.

[37] P. Seema, S.S. Swathy, M. Indira, Protective effect of selenium on nicotine-induced testicular toxicity in rats, Biol. Trace Elem. Res. 120 (2007) 212–218.

[38] C. Jalili et al., Protective effect of gallic acid on nicotine-induced testicular toxicity in mice, Pharm. Biol. 55 (2017) 1797–1803.